CHAPTER II
LITERATURE REVIEWS

2.1 Forest Carbon Pools

A forest ecosystem is one of the big carbon pools in the globe because of the capability to store carbon in various pools. There are seven standard carbon pools in a forest (**Table 2.1**) including: 1) aboveground biomass (AGB), all living biomass above the soil (e.g., stem, branches, seeds, foliage, and living understory plants); 2) belowground biomass, all living root biomass of plants; 3) deadwood, all dead woody biomass (either standing, down, or in the soil); 4) floor litter biomass, the dead biomass of leaves, twigs, needles, and others that lying on the ground and not yet become part of the soil by decomposition (with the diameter less than 7.5 centimeters); 5) soil carbon, all carbon-based material in soil including small-sized roots; 6) harvested wood products in use, which are currently being used (e.g., paper, boards, poles, and wood chips); and 7) harvested wood products in solid waste disposal sites, where they may eventually degrade and release their stored carbon, or remain intact for extended periods (Environmental Protection Agency (EPA), 2020; Hoover and Riddle, 2020). In tropical forests, AGB is a parameter for characterizing forest ecosystems and investigating production potential (Behera, Sahu, Mishra, Bargali, Behera, and Tuli, 2017).

Table 2.1 The types of carbon pools from forest ecosystem.

Type of the forest biomass	Standard forest pools
1 In part of the forest ecosystem	Aboveground biomass
	Belowground biomass
	Deadwood
	Floor litter biomass
	Soil carbon
2 Transported out of the forest ecosystem	Harvested wood products in use
	Harvested wood products in solid waste disposal sites

2.2 Basic Knowledge on Mangrove Forest

2.2.1 The Definition

Mangrove forests (also called mangrove swamps or mangals) are forests that are distributed in tropical and subtropical tidal areas, along estuaries and marine shorelines (Mathias, 2012). Mangrove forests are ecologically defined as the assemblages of trees and shrubs growing in the intertidal zone (foreshore). They include two components: 1) mangrove vegetation (mangrove forest) and 2) associated water bodies. The mangrove forest and associated water bodies are together called "mangrove wetland" (**Figure 2.1**). During the monsoon season, most of the mangrove wetlands are inundated by low saline water, and sometimes freshwater, brackish water, or sea water during other periods (Selvam and Karunagaran, 2019).

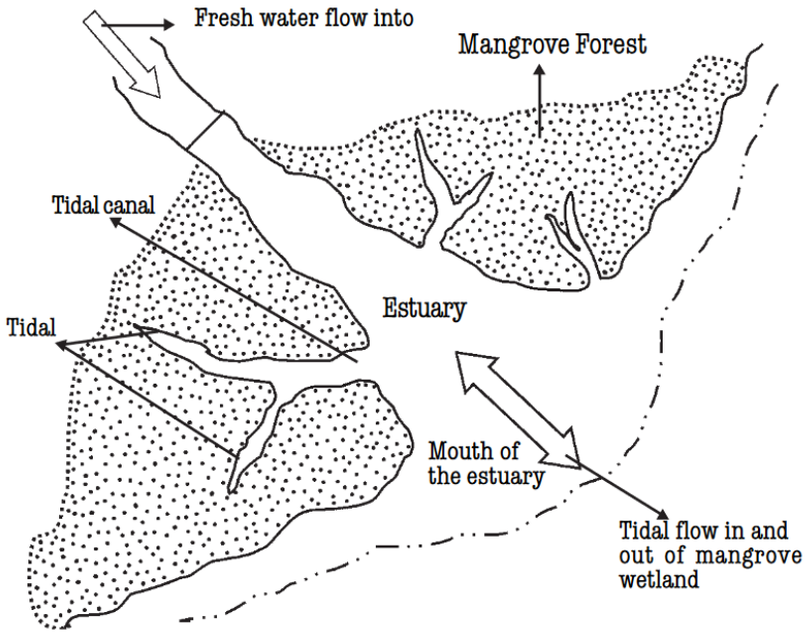

Figure 2.1 Mangrove wetland diagram (Selvam and Karunagaran, 2019).

2.2.2 Mangrove Plant Adaptation

The conditions of mangrove ecosystems are characterized by regular tidal inundation, elevated salinity levels, and reduced oxygen. The soil can be different in each place (firm, muddy, or slushy), besides, muddy and slushy can produce hydrogen sulfide (a gas with a rotten egg smell) showing that waterlogged soils are entirely

anaerobic. On some shorelines, the mangrove forests show distinct zonation because each mangrove species has a different adaptation. Small environmental variations may lead each species to have different strategies to overcome the environment. The mix of mangrove species can be influenced by the tolerances of each species to physical conditions (such as salinity and tidal flooding) and biological conditions (such as crabs feeding on seedlings) (Cannicci, Fusi, Cimó, Dahdouh-Guebas and Fratini, 2018; Selvam and Karunagaran, 2019). The convergent evolution, which happens in several plant families, causes mangroves to be taxonomically diverse. Mangroves grow worldwide mainly between latitudes 30°N and 30°S (cover tropical, subtropical, and some temperate coastal areas), however, the greatest mangrove areas are within 5° of the (Friess and Webb, 2014; Giri, Ochieng, Tieszen, Zhu, Singh, Loveland, Masek, and Duke, 2011).

Mangrove plants' adaptation to their environments contributes to the distinctive appearance of the vegetation. Each mangrove species can grow in different zones. Theoretically, five salinity zones can be accounted for horizontally in mangrove wetlands based on salinity distribution including: euhaline, polyhaline, mesohaline, oligohaline, and limnetic zone (**Table 2.2**). For example, in the Australian mangrove, it was found that *Avicennia marina* can grow in a broad range of salinity; *Sonneratia alba* grow in only euhaline zones; *A. integra* grow in polyhaline and mesohaline zones, while *S. lanceolata* grow in mesohaline and oligohaline zones (**Figure 2.2**). In addition, physical adaptation can be noticed in mangroves, such as looping stilt roots, needle-like aerial roots, and evergreen with shiny leaves. Moreover, mangrove canopy height is affected by climate, topography, and human disturbance. The mature undisturbed mangrove forest grows a high, dense canopy with tall trunks. The canopy is monotonous due to the relatively similar size, shape, and texture of the mangrove leaves. Besides, mangrove plants can become stunted and scrubby in a disturbed environment (Selvam and Karunagaran, 2019).

Table 2.2 The salinity range in different estuarine zones.

Zone	Range of salinity
Euhaline	> 30%
Polyhaline	18 - 30%
Mesohaline	5 - 18%
Oligohaline	0.5 - 5%
Limnetic	< 0.5% (fresh water)

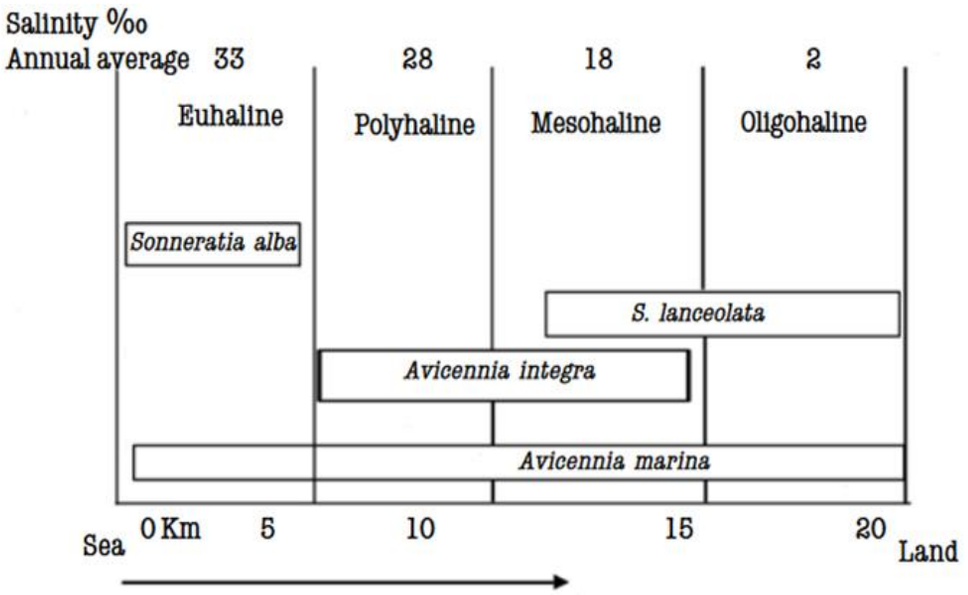

Figure 2.2 Distribution of mangrove species in an Australian mangrove in different salinity zones (Selvam and Karunagaran, 2019).

2.2.3 Mangrove Forest in the Sundaic Region

The three distinct biogeographic regions are located in Southeast Asia, which are Indochina, the Sundaic region (Sundaland), and the Philippines (Woodruff, 2010). The Sundaic region has seen rapid and severe mangrove degradation (Friess, Rogers, Lovelock, Krauss, Hamilton and Lee et al., 2019; Thomas, Lucas, Bunting, Hardy, Rosenqvist, and Simard, 2017). The region covers a part of southern Thailand,

Malaysia, Indonesia, Sumatra Island, Borneo Island, Java Island, and Bali Island. **Figure 2.3** illustrates the mangrove area in the Sundaic region, Southeast Asia. The mangroves, which are in the Sundaic region, consist of 58 genera and 69 species that are three times more diverse than mangroves in the Atlantic East Pacific zone (Saenger, Ragavan, Sheue, López-Portillo, Yong, and Mageswaran, 2019). This region is the center of key mangrove genera, including *Avicennia*, *Bruguiera*, *Ceriops*, *Lumnitzera*, *Rhizophora*, and *Sonneratia* (Chapman, 1977).

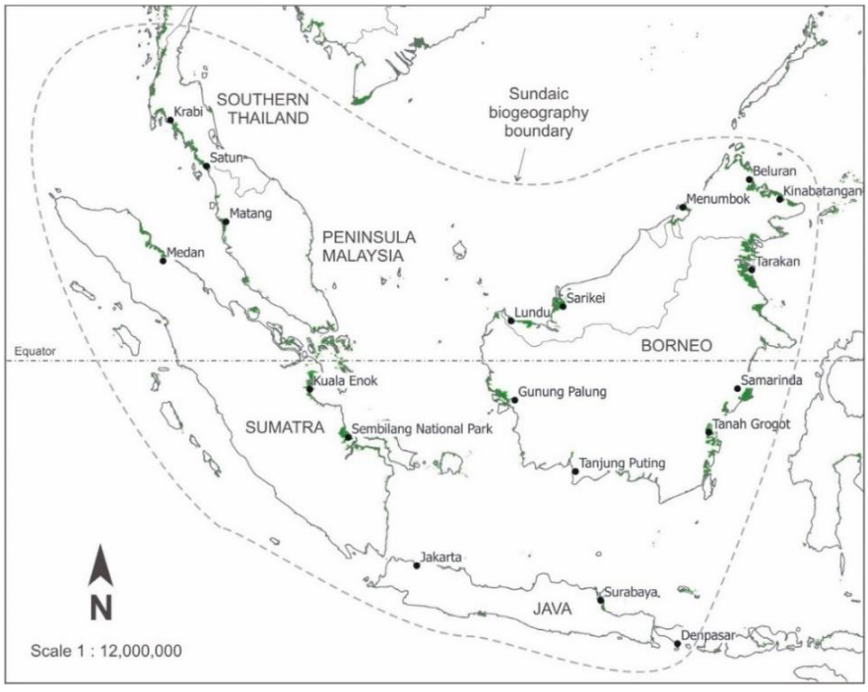

Figure 2.3 The Sundaic biogeographical region (dashed line) and its mangrove area (Bunting et al., 2018; Ng and Ong, 2022; Woodruff, 2010).

2.2.4 Mangrove Carbon Storage in the Sundaic Region

In the Sudanic region, the carbon storage in the mangrove ecosystem is exceptionally high compared to other world's major forests (**Figure 2.4**). Donato, Kauffman, Murdiyarso, Kurnianto, Stidham, and Kanninen (2011) found that the mangrove ecosystem contains an average carbon stock of 1,023 ± 88 Mg C ha^{-1}, which is three to five times more carbon (C) per unit area compared with boreal, temperate, and tropical upland forests, with rich organic sediment accounting for 49 to 98% of the carbon storage.

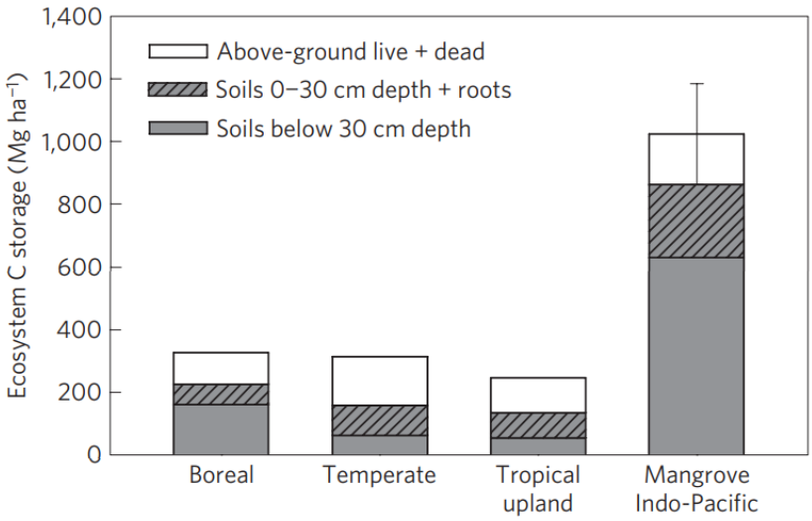

Figure 2.4 Comparison of mangrove carbon storage with different global forest domains (Donato et al., 2011).

2.2.5 Mangroves in Thailand

Mangroves in Thailand are found on mudflats at river mouths and along the country's eastern and southern coastlines, particularly along the Andaman Sea and the Gulf of Thailand. (**Figure 2.5**). In addition, the mangrove families are distributed in the Chao Phraya Delta. Typically, the mangroves form two stories: 1) the upper layer (grows to 20 m in height) that is dominated by *R. apiculata, R. mucronata, Heritiera littoralis, and Xylocarpus mekongensis*; whereas the lower layer is commonly dominated by *Bruguiera cylindrica*, *B. parviflora, B. sexangula*, *Ceriops decandra*, and *C. tagal*). However, *B. gymnorrhiza* can grow 40 m in height (above the forest) with 2 m in girth. Near the land where mud accumulates, drier soil supports the growth of ferns and herbs, forming evergreen forests. The chak palm, *Nypa fruticans*, is commonly found along creek edges (FAO, 2005). Mangrove species are influenced by their location, which is affected by the chemical and physical properties of the sediment, salinity levels, water drainage and current, sediment moisture, and the frequency of flooding (Aksornkoae, 1999). In 1975, mangroves in Thailand covered about 320,000 hectares. However, by 1996, this area had decreased to around 160,000 hectares. Due to the conservation and rehabilitation efforts in Thailand, the mangrove area increased to

240,000 hectares by 2004 (Pumijumnong, 2014). By the year 2020, the mangrove area had expanded to over 601,642 hectares. (Bajaj et al., 2024).

Mangroves in Thailand have faced a variety of challenges. These challenges include: 1) the remaining mangrove areas, which are continuously utilized by local inhabitants, particularly evident along the Andaman coastline in Ranong, Krabi, Trang, Satun, and Phuket; 2) the encroachment of mangrove areas by shrimp farmers in the eastern Thai Gulf and in the provinces of Chantaburi, Surat Thani, and Nakhon Si Thammarat; 3) the sale of mangrove land titles prompted by losses from prior utilization. Additionally, improper land use continues to contribute to coastal erosion, particularly in the provinces of Samut Prakarn, Samut Sakhon, Samut Songkhram, Phetchaburi, and Chacheongsao. In 2007, using remote sensing technology and interpreting LANDSAT 5 satellite images, the mangrove area in Thailand was estimated to cover 1,435,116 Rai, with the largest portion in Phang Nga province, accounting for 18.55% of the total mangrove area in the country (Pumijumnong, 2014).

Figure 2.5 The distribution of mangrove along coastline of Thailand (Elwin, 2020).

2.2.6 Mangrove Forest in Nakhon Si Thammarat

The official website of the Department of Marine and Coastal Resources (Department of Marine and Coastal Resources, 2018), indicated that the mangrove area, in Nakhon Si Thammarat province, Southern Thailand, is approximately 80,922.14 rai (12,947.54 ha). The mangroves are distributed in four different districts: 1) Mueang Nakhon Si Thammarat district, 2) Khanom district, 3) Tha Sala district, and Pak Phanang district. The mangrove species with the highest density were tall-stilt mangrove (*Rhizophora apiculata*), cannonball mangrove (*Xylocarpus granatum*), and loop-root mangrove (*Rhizophora mucronata*) with respective weights of 47, 36, and 30 tons/rai. The highest average mangrove tree heights were recorded for the mangrove apple (*Sonneratia alba*) at 12.5 meters, followed by the sunder (*Heritiera fomes*) at 12.5 meters, the crabapple mangrove (*Sonneratia caseolaris*) at 12.03 meters, and the Indian mangrove (*Avicennia officinalis*) at 10.93 meters.

2.3 Estimation of Forest Biomass

Various methods have been developed to estimate forest biomass. Shi and Liu (2017) showed the comparison of different measurement methods including allometric equation, mean biomass density, biomass expansion factor, forest identify, remote sensing, and geostatistics (**Table 2.3**). Each method is appropriate to different forest scales including: 1) individual or stand (allometric equation), 2) stand (biomass expansion factor), 3) stand or region (mean biomass density and remote sensing), and 4) region (forest identity and geostatistics). Each technique has its limitations and improvement practices, for example, the allometric-equation method has limitations in terms of less sampling trees, and improvement practices in terms of incorporating other factors into allometric coefficients.

Table 2.3 Comparison of the estimation methods of forest biomass (Shi and Liu, 2017).

Scale	Method	Limitation	Improvement practices
Individual or stand	Allometric equation	Varying with many factors (species, terrain, temperature, and rainfall); less sampling of trees	Incorporating other factors into the allometric coefficient, such as combining with LIDAR
Stand	Biomass expansion factor	Varying with many factors (species, terrain, temperature, and rainfall)	Incorporating other factors into the conversion factor
Stand or region	Mean biomass density	Leading to an overestimation	More random plots
	Remote sensing	Saturation and bidirectional reflectance from surface features	Finer spatiotemporal resolution, advanced technology, and algorithm
Region	Forest identity	The requirement for comprehensive analysis	-
	Geostatistics	The requirement for more field data	Creating of biomass database

Note:

Allometric equation: the equation that is used to estimate the ecological factors (such as biomass) by measuring the diameter at breast height (DBH) and/or height of trees.

Biomass expansion factor (BEF): the estimation of forest biomass based on the assumption that there is a certain relationship between the growing stock and biomass;

thus, the forest biomass can be estimated based on BEF conversion factor multiplied by the growing stock (derived from national forest inventory (NFI), for example).

Mean biomass density: the estimation of stand or forest biomass by the area multiplied by the mean biomass density.

Remote sensing (RS): the applying of RS in biomass estimation, such as the use of normalized difference vegetation index (NDVI)

Forest identity: the use of measurable variables and integrating their changes quantitatively and logically into a relationship.

Geostatistics: the applying of various types of spatial phenomena, such as climate, physicalness, and other natural disturbances, to study nature (including forest biomass).

2.4 Remote Sensing (RS)

2.4.1 Basic Knowledge of Remote Sensing

Remotely sensed data provide an effective solution to the challenges of traditional field-based methods. Their key benefits—such as frequent data acquisition, a broad perspective, digital format allowing for quick processing of large datasets, and strong correlations between spectral bands and vegetation variables—make them a primary tool for AGB across vast regions. (Lu, 2006). Advances in space-borne and air-borne RS technologies are increasingly being used to obtain fast, reliable, and consistent data over extensive areas (Saukkola, Melkas, Riekki, Sirparanta, Peuhkurinen, and Holopainen et al., 2019).

RS can generally be divided into two categories (Campbell and Wynne, 2011; Lillesand, Kiefer and Chipman, 2015), according to **Figure 2.6**: 1) passive remote sensing, this method detects natural radiation emitted or reflected by an object or its surroundings, with sunlight being the most common source, optical sensors are frequently employed in passive remote sensing; 2) active remote sensing: this approach involves sending energy towards a target and analyzing the energy that is reflected to the sensor. Examples of active remote sensing technologies include Radio Detection and Ranging (RADAR) and Light Detection and Ranging (LiDAR).

Both passive and active remote sensing possess distinct advantages and disadvantages. Passive remote sensing provides numerous benefits, such as abundant data acquisition, ease of interpretation, cost-efficiency, minimal environmental interference, and the ability to measure temperature. However, it also has notable limitations, including high sensitivity to weather conditions and reduced effectiveness in low-light or nighttime environments (Shangari, Shams, Azari, Shamshirdar, Baltes, and Sadeghnejad, 2017). Active remote sensing is known for its high accuracy in both lateral and longitudinal measurements, its capability to determine target distances, and its independence from sunlight. However, it also has some limitations, including high costs, complex interpretation, and sensitivity to weather conditions (Shangari et al., 2017).

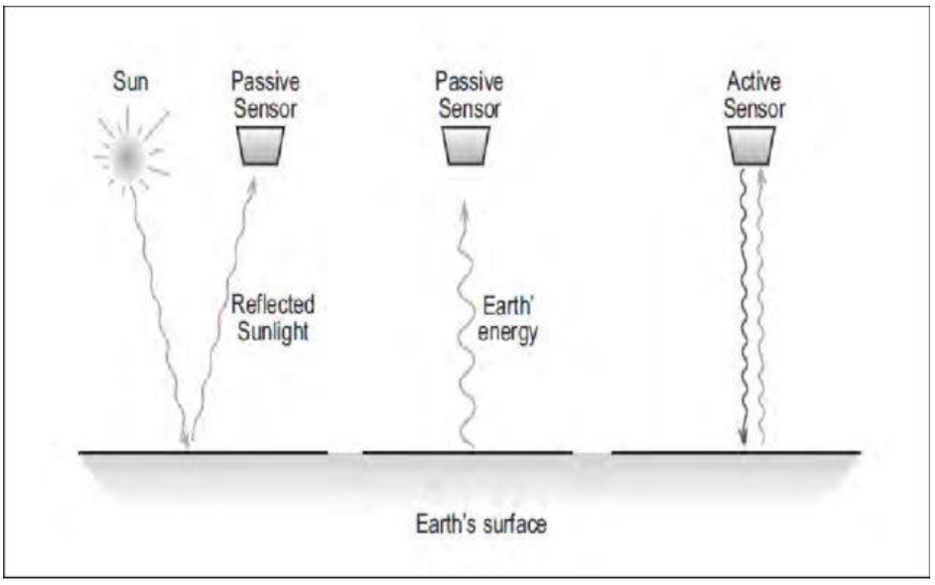

Figure 2.6 Passive and active remote sensing (Sourav, 2017).

2.4.2 Unmanned Aerial Vehicles (UAVs)

The UAVs or drones have attracted considerable interest in recent years because of their diverse applications in areas such as agriculture, surveillance, environmental monitoring, and disaster management. This increasing focus on UAVs is largely due to technological advancements that have enhanced their functionalities, including improved sensors, greater autonomy, and more efficient communication systems (Colomina and Molina, 2014). UAVs can be utilized in smart agriculture to

gather specific data via ground sensors (such as water quality, soil composition, humidity, and more), apply pesticides, diagnose diseases, schedule irrigation, identify weeds, and oversee crop management. The use of drones in precision agriculture is a cost-effective and time-efficient approach that can enhance the revenue, performance, and overall productivity of agricultural systems (Mohsan, Othman, Li, Alsharif, and Khan, 2023). Moreover, UAVs fitted with multispectral sensors offer the ability to monitor vegetation with high spatial and temporal resolution as needed (Easterday, Kislik, Dawson, Hogan, and Kelly, 2019).

2.5 Vegetation Indices (VIs)

Vegetation indices are numerical measures derived from reflective data captured by satellite or airborne sensors to assess the condition and quality of vegetation in a given region. These indices are crucial in agriculture, forestry, environmental monitoring, and land-use planning. Among the numerous vegetation indices, the Normalized Difference Vegetation Index (NDVI), Soil-Adjusted Vegetation Index (SAVI), and Green Normalized Difference Vegetation Index (GNDVI) are commonly applied in environmental and agricultural monitoring. Each of these indices tackles challenges in vegetation analysis, including issues related to soil brightness and the structure of the plant canopy. Some study utilized these indices to evaluate their effectiveness in developing models for mangrove AGB (Nguyen et al., 2019).

2.5.1 Normalized Difference Vegetation Index (NDVI)

The NDVI is the most frequently utilized vegetation index due to its ease of use and adaptability. Healthy vegetation reflects a significant amount of NIR light while absorbing red light, leading to higher NDVI values (usually between 0.2 and 0.8 for areas with vegetation). NDVI is widely used in land cover classification, monitoring vegetation health, and evaluating agricultural productivity. It serves as a vital tool for observing changes in vegetation, such as deforestation, desertification, and seasonal growth trends (Tucker, 1979). A significant limitation of the NDVI is its sensitivity to soil background and atmospheric conditions, which can distort results in regions with sparse vegetation or inconsistent soil reflectance (Huete, 1988).

It is calculated using the following formula:

$$\mathrm{NDVI} = \left(\frac{\mathrm{NIR}-\mathrm{RED}}{\mathrm{NIR}+\mathrm{RED}}\right)$$ Zaitunah, Samsuri, Ahmad, and Safitri (2018)

Where: NIR is the reflectance in the near-infrared region, and RED is the reflectance in the red portion.

2.5.2 Soil-Adjusted Vegetation Index (SAVI)

The SAVI is developed to overcome the limitations of NDVI in regions with sparse vegetation, where soil reflectance can significantly affect the NDVI accuracy. This index was introduced to reduce the impact of soil brightness on spectral vegetation indices that involve red and near-infrared (NIR) wavelengths (Huete, 1988).

It is calculated using the following formula:

$$\mathrm{SAVI} = \left(\frac{\mathrm{NIR}-\mathrm{RED}}{\mathrm{NIR}+\mathrm{RED}+\mathrm{L}}\right) \times (\mathrm{L}+1)$$ Huete (1988)

Where: L is a constant that ranges from 0 to 1, with lower values assigned to denser vegetation and higher values for sparser vegetation. A common value for L is 0.5, which has proven effective in balancing soil influence and the vegetation signal (Huete, 1988).

2.5.3 Green Normalized Difference Vegetation Index (GNDVI)

The GNDVI is a modified version of NDVI that utilizes green light reflectance instead of red light, providing improved sensitivity to chlorophyll levels in plants. In comparison to NDVI, GNDVI is more responsive to changes in plant health related to chlorophyll content, particularly in crops and grasses (Gitelson Kaufman and Merzlyak, 1996).

It is calculated using the following formula:

$$\mathrm{GNDVI} = \left(\frac{\mathrm{NIR}-\mathrm{GREEN}}{\mathrm{NIR}+\mathrm{GREEN}}\right)$$ Gitelson et al. (1996)

Where: GREEN is the reflectance in the green portion.

2.6 Related Studies in Mangrove Biomass and Carbon Stock

Estimations of mangrove biomass and carbon stock have been performed using various techniques. Over the past five years (2019-2023), both conventional methods (destructive and allometric) and remote sensing techniques have continued to be utilized. Southeast Asia (SEA) is one of the regions that has been the focus of studies on mangrove biomass and carbon stock. **Table 2.4** presents a summary of some literature reviews related to the assessment of mangrove biomass and carbon stock.

2.6.1 The Related Studies of RS to Mangrove AGB Model in Thailand

In Thailand, a study was identified that developed mathematical models to estimate the AGB and AGC stock in mangrove forest. The study evaluated mangrove biomass along Thailand's Andaman Coast by integrating high-resolution GeoEye-1 satellite imagery, medium-resolution ASTER satellite elevation data, field-based tree measurements, existing allometric biomass equations, vegetation indices, and advanced machine learning techniques (Jachowski, Quak, Friess, Duangnamon, Webb, and Ziegler, 2013). The research successfully developed spatial models to estimate mangrove biomass with an R^2 of 0.66 to estimate the mangrove AGB (Jachowski et al., 2013).

Table 2.4 Related studies in the estimation of mangrove carbon stocks.

No	Technique	Methodology	Finding	Location	References
1	Allometric equation and destructive samplings	The sample trees (different age classes and diameter sizes) were cut down and then measured the fresh biomass. The dry biomass and carbon content were analyzed in the laboratory. The linear functions were applied to generate models (allometric equations) for the mangrove AGB estimation.	The generated models formed a high R^2 (0.85 – 0.99) with the mangrove biomass. The carbon stock in forest biomass ranged from 23.8 to 188.7 tons C/ha (117.4 tons C/ha in average).	Ca Mau Province, Vietnam	Quang, Thi, Nguyet, Hoan, Viet, and Hung (2022)
2	Allometric equation and sample collection	Sampling the mangrove ecosystem components (root, litter, downed wood, and soil) to analysis in the laboratory, whereases the mangrove tree biomass was measured with allometry.	The total ecosystem carbon stock ranged from 168.27 to 296.45 tons/ha. The most carbon fraction is in sediment (168.27 – 243.87 tons/ha), followed by tree (0 – 66.20 tons/ha), respectively.	Along the Straits of Malacca between Merlimau and Kuala Sebatu in Jasin, Malacca, Malaysia	Safwan, Mohd, Sharma, Liyana, Mohamad, Palaniveloo, and MacKenzie (2023)

Table 2.4 (Continued).

No	Technique	Methodology	Finding	Location	References
3	Remote Sensing (Satellite imagery)	The AGB was estimated by using linear regression between vegetation indices (NDVI, SAVI, and GNDVI) and AGB from ground truth data. The vegetation indices were calculated from satellite imageries (Landsat and Sentinel-2).	All the tested vegetation indices (NDVI, SAVI, and GNDVI) had a high coefficient of determination (R^2 = 0.68). The mangrove AGB was 22.57 tons/ha (1998) and 37.74 (2018) ton/ha with the total change of 15.17 ton/ha.	Thai Binh Province coastal area and Xuan Thuy national park (Giao Thuy district - Nam Dinh province), that is part of the Red River Delta of Vietnam	Nguyen et al. (2019)
4	Remote Sensing (Satellite imagery)	The AGB was estimated by AGB estimation model through stepwise linear regression approaches between spectral bands/vegetation indices and AGB from ground truth data. The spectral bands and vegetation indices were calculated from satellite imageries (Landsat-8 and Sentinel-2).	The models based on Sentinel-2 spectral bands and vegetation indices (R^2 > 0.855) were more accurate in estimating the overall AGB of mangrove forests than those based on Landsat-8 data.	Mong Cai, a coastal city of Quang Ninh Province in the Red River Delta region of Vietnam	Nguyen and Nguyen (2021)

Table 2.4 (Continued).

No	Technique	Methodology	Finding	Location	References
5	Remote Sensing (UAV imagery)	For the aerial imagery, the tree height and number of branches were calculated using a Digital Surface Model (DSM) corrected by a digital elevation model (DEM). Then, the mangrove biomass was estimated with an allometric equation that only uses height as the parameter.	The tree's height ranges from 1 to 15.5 meters, with an average height of 4.4 meters. The estimated mangrove biomass was 82,154 tons/ha.	Karimunjawa National Park, Jepara Regency, Central Java Province, Indonesia	Salim, Adi, Kepal, and Ati (2020)
6	Remote Sensing (UAV imagery)	Tree detection and canopy segmentation algorithms were applied to Structure from Motion and Multi-View Stereo reconstructions from Unmanned Aerial Vehicles imagery (UAV-SfM) data to estimate AGB.	The comparison of ground AGB estimates to UAV-SfM derived estimates using all data and only top canopy provided a strong correlation (*adjusted* R^2 of 0.932 and 0.91, respectively).	the southeastern coast of Australia including: 1) Western Port, Victoria and 2) Richmond River Estuary, New South Wales	Navarro, Young, Allan, Carnell, Macreadie, and Ierodiaconou (2020)

Table 2.4 (Continued).

No	Technique	Methodology	Finding	Location	References
7	Remote Sensing (UAV imagery)	The mangrove canopy height was calculated by subtracting Digital Surface Model (DSM) from Digital Terrain Model (DTM), then converting the canopy height to Lorey's height using exponential regression with the mangrove survey data. The AGBs were calculated using an allometric equation, then converted to above-ground carbon by multiplying with 0.5	The regression model to estimate mangrove Lorey's height shows a good accuracy (bias and RSME of 0.04 m and 1.28 m, respectively).The mangrove AGB and carbon stock range from 8 tons/ha to 328 tons/ha, and from 4 tons/ha to 164 tons/ha, respectively.	Karimunjawa Islands, Indonesia	Wirasatriya, Pribadi, Iryanthony, Maslukah, Sugianto, Helmi et al. (2022)